JOURNAL OF MATERIALS SCIENCE **39** (2004) 587–591

Effects of thickness on fatigue properties of investment cast Ti-6Al-4V alloy plates

JINKEUN OH, JUNG GU LEE, NACK J. KIM, SUNGHAK LEE, EUI W. LEE*
Center for Advanced Aerospace Materials, Pohang University of Science and Technology, Pohang 790-784, Korea
E-mail: shlee@postech.ac.kr

The present study is concerned with the effects of plate thickness on high-cycle fatigue properties and fatigue crack propagation behavior of investment cast Ti-6Al-4V alloys having Widmanstätten structure. High-cycle fatigue test and fatigue crack propagation test were conducted on three cast plates having different thickness, and then the test data were analyzed in relation with microstructures, tensile properties, and fatigue fracture mode. The high-cycle fatigue results indicated that fatigue strength of the three cast plates was quite similar because of their similar tensile strength. In the case of the fatigue crack propagation, the thicker cast plate composed of thinner α platelets had the slightly faster crack propagation rate than the other plates. The effective microstructural factor determining the fatigue crack propagation rate was found to be the thickness of α platelets because it was well matched with the reversed cyclic plastic zone size calculated in the threshold ΔK regime.

1. Introduction

A Widmanstätten structure of a Ti-6Al-4V alloy is known to have excellent specific strength, fracture toughness, and resistance to crack propagation [1], and is typically composed of colonies in which thin α platelets are aligned in a β matrix. A typical example of the Widmanstätten structure is a cast Ti-6Al-4V alloy made by an investment casting method which has been used as an excellent technology to fabricate complicated airplane parts. This investment cast Ti-6Al-4V alloy must have excellent fatigue properties so that it can be used for airplane parts. Fatigue properties of titanium alloys are largely determined by surface defects [2], microstructures [3], and crystallographic textures [4]. There generally exist many cast defects such as micropores inside investment cast parts, but most of them can be removed by a hot isostatic pressing (HIP) process. Fatigue properties are also affected by microstructural factors such as size and morphology of β grains, colonies, and α platelets [5–12], but systematic studies on how microstructural factors affect fatigue properties of the investment cast Ti-6Al-4V alloy are yet to be made. In the present study, three kinds of Ti-6Al-4V alloy plates having different thickness were fabricated by investment casting, and their fatigue properties were investigated. Effects of microstructural factors on fatigue properties were analyzed by observing the fatigue crack propagation behavior and fracture surfaces.

2. Experimental

The materials used in this study were three kinds of investment cast Ti-6Al-4V plates of 6, 13, and 19 mm in thickness, which were manufactured at Howmet Corp., Whitehall, MI, U.S.A. Chemical compositions of the plates were measured by an inductively coupled plasma (ICO) analysis method, and the results are shown in Table I. The plates were HIP'ed at 900°C for 2 h under a pressure of 103 MPa, and were annealed at 843°C for 2 h.

After the plates were etched by a Kroll solution (H_2O 100 ml, HF 3 ml, and HNO_3 5 ml), they were observed by an optical microscope and a scanning electron microscope (SEM). Prior β grain size, colony size, and α platelet size were measured from optical and SEM micrographs using an image analyzing program (sigmascan). Plate-type tensile specimens with a gage section (length: 11.8 mm, thickness: 1.8 mm, width: 5 mm) were machined, and room-temperature tensile tests were conducted at a strain rate of 6.4×10^{-4} sec^{-1}.

Fig. 1a exhibits the shape and dimensions of an hourglass-shaped fatigue specimen. Room-temperature high-cycle fatigue test was conducted at a stress ratio $R(=P_{\min}/P_{\max}) = 0.1$ using sinusoidal loading at a cyclic frequency of 20 Hz. The test was conducted to obtain S-N curves, from which fatigue strength was measured at 10^7 cycles. Using a compact tension specimen in which a machined notch was inserted (Fig. 1b), fatigue crack propagation test was also performed under

**Present address:* Code 4342, Naval Air Warfare Center, Patuxent River, MD 20670, USA.

TABLE I Chemical composition of the three investment cast Ti-6Al-4V plates having 6, 13, and 19 mm thickness

Plate	Al	V	Fe	C
6 mm thick	5.87	4.02	0.51	0.03
13 mm thick	5.88	4.02	0.53	0.03
19 mm thick	5.84	4.11	0.53	0.02

the same conditions of the high-cycle fatigue test (room temperature, $R = 0.1$ and 20 Hz cyclic frequency). The crack lengths were measured using a traveling microscope, and the fatigue crack closure load was measured by a compliance method using a crack opening displacement gage [13]. After the fatigue tests, fractured surfaces were observed in an SEM.

3. Results and discussion

3.1. Microstructure and tensile properties

Fig. 2a through f are optical micrographs of investment cast Ti-6Al-4V plates. Prior β grain size ranges from 800 to 900 μm in the 6-mm-thick plate, and increases to over 1 mm in the 13- and 19-mm-thick plates. Prior β grains are composed of several colonies (Fig. 2a through c). The colony size increases with increasing the plate thickness, and that of the 19-mm-thick plate ranges from 600 to 700 μm, which is about twice over that of the 6-mm-thick plate. The colony is composed of a Widmanstätten structure of α and β platelets as shown in Fig. 2d through f. The thickness of α platelets ranges from 3 to 4 μm. This tends to increase slightly with increasing the plate thickness. β platelets of several hundred nanometers in thickness are continuously formed between α platelets, and grain boundary α phases having 6–8 μm thickness are also observed, as indicated by arrows. Microstructural factors were quantitatively analyzed, and the results are shown in Table II.

The room-temperature tensile test data are listed in Table III. Yield and tensile strengths of the three plates are similar in the range of 870–880 MPa and 910–920 MPa, respectively, and slightly increase with increasing the plate thickness. However, elongation decreases as the plate thickness increases.

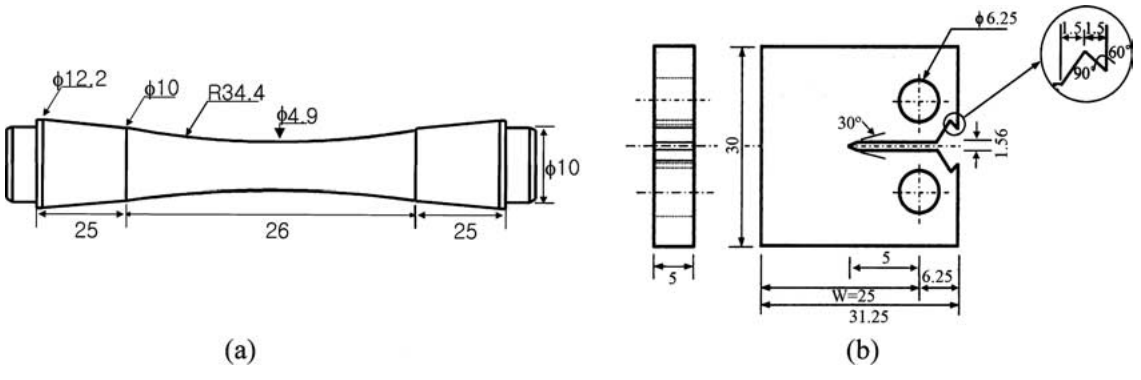

Figure 1 The shape and dimensions of (a) an hourglass-shaped high-cycle fatigue specimen and (b) a compact tension specimen used for the fatigue crack growth rate measurement. (unit: mm)

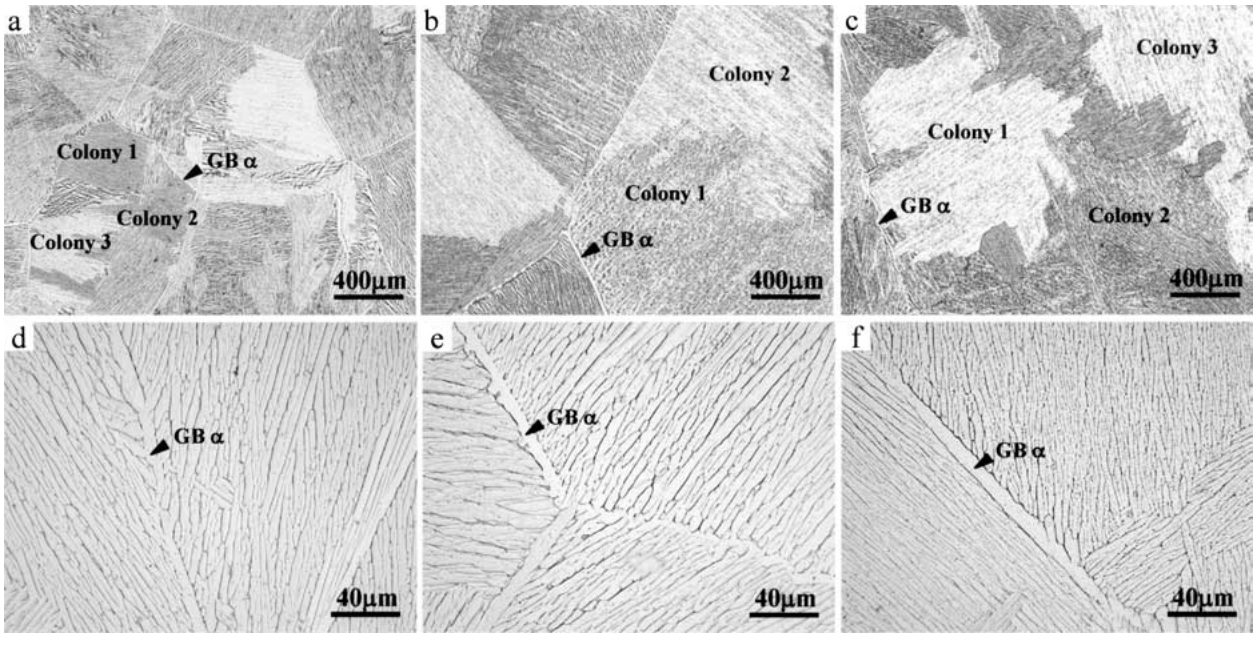

Figure 2 Optical micrographs of the (a) and (d) 6-, (b) and (e) 13-, and (c) and (f) 19-mm-thick plates. Kroll etched.

TABLE II Quantitative analysis data of the three investment cast Ti-6Al-4V plates having 6, 13, and 19 mm thickness

Plate	Prior β gain size (μm)	Colony size (μm)	GB α phase thickness (μm)	α platelet thickness (μm)
6 mm thick	840	384	8.6	3.61
13 mm thick	1553	565	7.5	3.51
19 mm thick	2050	652	6.5	3.07

TABLE III Room-temperature tensile test results, threshold ΔK, and calculated reversed plastic zone size

Plate	Yield strength (MPa)	Tensile strength (MPa)	Elongation (%)	Threshold $\Delta K(\Delta K_{th})$ (MPa$\sqrt{m}$)	Transitional reversed plastic zone size (μm)
6 mm thick	867	908	11.1	7.74	4.2
13 mm thick	880	919	9.0	7.70	4.0
19 mm thick	884	922	8.2	7.57	3.9

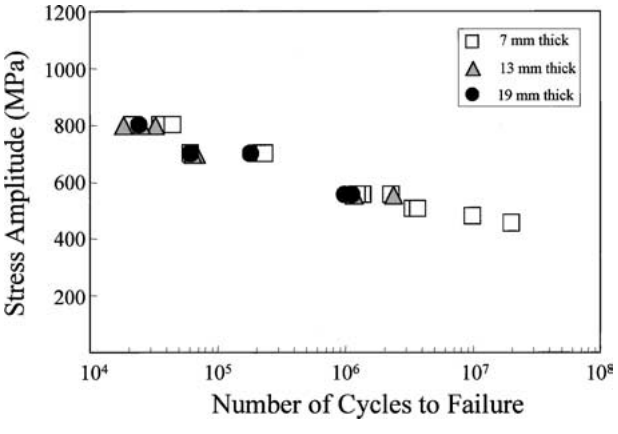

Figure 3 S-N curves of the investment cast plates.

3.2. Fatigue properties

Fig. 3 shows the room-temperature high-cycle fatigue test results. Fatigue strength (at 10^7 cycles) of the three plates is similar (about 500 MPa), regardless of the plate thickness. The fatigue limit from the viewpoint of small cracks is the fatigue strength at which the small cracks grow to be long cracks by overcoming some obstacles such as grain boundaries. The main obstacles in this study are thought to be α/β boundaries, and the α platelet thickness is similar in the three plates (Table II), thereby leading to the similar fatigue strength in the three plates.

Fig. 4a is an SEM fractograph showing the overall high-cycle fatigue fracture surface of the 6-mm-thick plate. A fatigue crack initiates near the surface as shown in a circled area of Fig. 4a. From a higher-magnification SEM fractograph of this circled area, it is found that a fatigue crack initiates at a prior β grain boundary and then propagates (Fig. 4b). These fractographic results match well with the results of other researchers [14–17].

In general, high-cycle fatigue life is dependent on the initiation and propagation of fatigue cracks. Since the crack initiation takes up much of the overall fatigue life when there are not many interior defects, it is required to find the crack initiation sites. It is known that fatigue cracking in a Ti-6Al-4V alloy starts at prior β grain boundaries or colony boundaries [15, 18, 19]. The present study also confirms that fatigue initiates mainly at prior β grain boundaries (arrow-marked in Fig. 4b). The sub-surface nucleation sites such as inclusions or defects are not observed here. Since the fatigue strength usually increases with increasing tensile strength [1], it is expected that the fatigue strength of the three plates is similar according to their similar tensile strength.

Fig. 5 shows the results of the fatigue crack propagation test. Resistance to fatigue crack growth is similar in the three plates. Threshold ΔK values (ΔK_{th} at 10^{-10} m/cycle) of the 6-, 13-, and 19-mm-thick plates are 7.74, 7.70, and 7.57 MPa$\sqrt{m}$, respectively, indicating that the increased plate thickness shows no significant change in ΔK_{th}. Fig. 6 shows the effect of the colony size and α platelets thickness on the ΔK_{th} value. ΔK_{th} decreases with increasing the colony size, which is contradictory to the results that ΔK_{th} is proportional to the colony size [6, 7]. ΔK_{th} increases with increasing the α platelet thickness. SEM micrographs showing fatigue crack propagation paths near the threshold ΔK regime of the 6-mm-thick plate are presented in Fig. 7a and b. Crack branching or secondary cracking are observed in

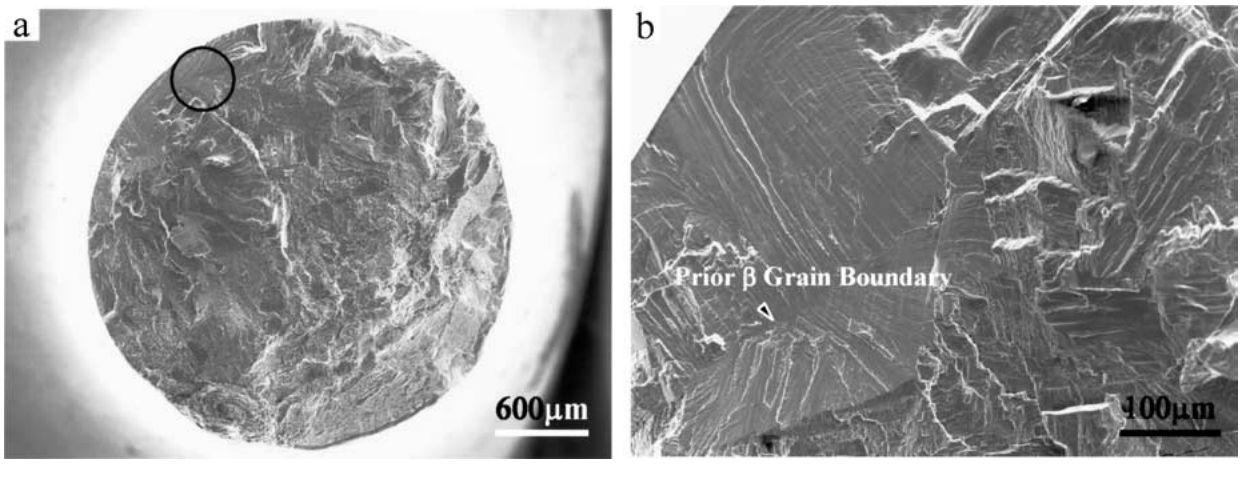

Figure 4 (a) and (b) SEM fractographs of the high-cycle fatigue specimens of the 6-mm-thick plate. (b) is a higher-magnification SEM fractograph of the circled area of (a), showing a fatigue crack initiation at a prior β grain boundary.

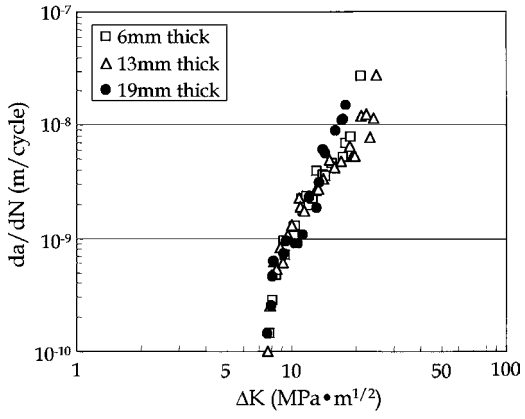

Figure 5 Fatigue crack growth behavior of the investment cast plates.

some areas (Fig. 7a), and the main propagating fatigue crack path is slightly changed as it passes through β platelets, as indicated by arrows in Fig. 7b.

It is noteworthy from Fig. 5 that the fatigue crack propagation rate changes near da/dN of 10^{-9} m/cycle. Based on this turning point, ΔK_T, the fatigue crack propagation rate of each plate shows a large difference in the case of $\Delta K < \Delta K_T$, whereas the difference decreases when $\Delta K > \Delta K_T$ [6]. The fatigue crack propagation rate at ΔK_T changes depending on how sensitive the fatigue crack propagation is to an effective microstructure [6–12]. The $\Delta K < \Delta K_T$ region is sensitive to microstructures, whereas the $\Delta K > \Delta K_T$ region is not. The effective microstructure in the $\Delta K < \Delta K_T$ region is known to be the colony size [6, 7]. Also, changes in the fatigue crack propagation rate in the $\Delta K < \Delta K_T$ region are reported to be related with the reversed cyclic plastic zone size, r_p, or the effective microstructure size [6–12]. When the former equals the latter which can be estimated as in the following equation [20], the fatigue crack propagation rate changes.

$$r_p = 0.318\left(\frac{\Delta K_{eff}}{2\sigma_y}\right)^2 \quad (\Delta K_{eff} = K_{max} - K_{cl})$$

ΔK_{eff} can be obtained from measuring the extent of roughness-induced crack closure. Table III provides the reversed cyclic plastic zone size calculated from the above equation. The reversed cyclic plastic zone is sized several micrometers, which match with the width of α platelets in Table II, although the r_p is somewhat larger than the α platelet width. In addition, β platelets located between α platelets work as retardation sites to crack growth at a lower ΔK region by slightly changing the fatigue crack propagation path (Fig. 7b). It is thus found that the effective microstructural factor governing the fatigue crack propagation at the lower ΔK region is not the prior β grain size or colony size, but is the α platelet width.

It is noted that the importance of α platelets has been almost ignored in view of the fatigue crack growth behavior as in many previous studies [4, 5]. In this study, however, it is suggested that the fatigue crack propagation behavior of the investment cast Ti-6Al-4V can be

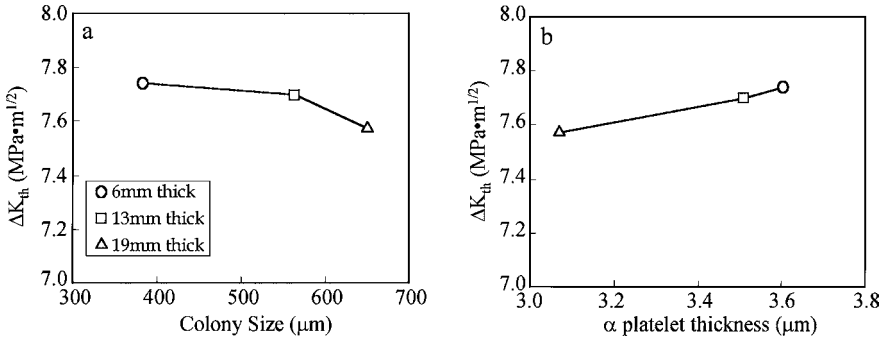

Figure 6 The variation of threshold fatigue crack growth as a function of colony size and α platelet thickness.

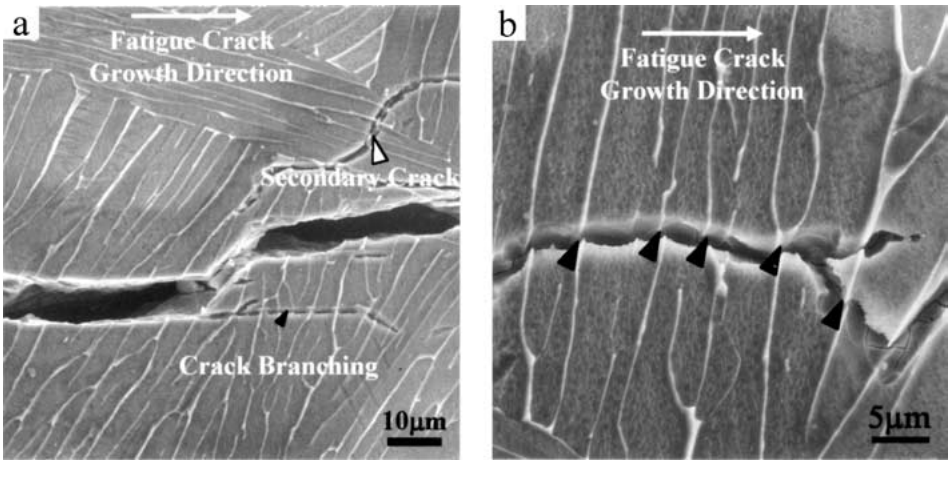

Figure 7 Fatigue crack propagation path observed at near-threshold ΔK for the 6-mm-thick plate, showing: (a) crack branching and secondary cracking and (b) path tortuosity at β platelets.

mainly affected by the thickness of α platelets. This is particularly important when the crack tip lies within a colony or the plastic zone size is similar to the thickness of platelets, while the colony size can also affect the fatigue crack growth when the crack propagates across colony boundaries.

4. Conclusions

The investment cast Ti-6Al-4V plates were composed of a Widmanstätten structure, and the size of prior β grains and colonies increased with increasing the plate thickness, while the thickness of α platelets and grain boundary α phases slightly decreased. Yield and tensile strengths of the plates were similar or slightly increased with increasing the plate thickness, whereas elongation was decreased. The high-cycle fatigue test results indicated that the fatigue strength of the three plates was similar according to the similar tensile strength, regardless of the plate thickness. In the case of the fatigue crack propagation, the thicker plate composed of thinner α platelets had the slightly faster crack propagation rate than the other plates. The effective microstructural factor determining the fatigue crack propagation rate was found to be the thickness of α platelets because it was matched with the reversed cyclic plastic zone size calculated in the threshold ΔK regime.

Acknowledgments

This work was supported by the U.S. Office of Naval Research under the contract No. N00014-98-1-0804. The authors would like to thank Mr. Stewart Veeck of Howmet Corp. for his help on the investment casting experiments.

References

1. G. LUTJERING, *Mater. Sci. Eng.* A **243** (1998) 32.
2. C. S. C. LEI, W. E. FRAZIER and E. W. LEE, *J. Metals* **49** (1997) 38.
3. S.-H. KIM and Y.-I. PARK, *Met. Mater.* **6** (2000) 133.
4. G. LUTJERING and A. GYSLER, *Titanium Sci. Tech.* **4** (1985) 2068.
5. M. PETERS, A. GYSLER and G. LUTJERING, *Metall. Trans.* A **15A** (1984) 1579.
6. G. R. YODER, L. A. COOLEY and T. W. CROOKER, *ibid.* **9A** (1978) 1413.
7. G. R. YODER and D. EYLON, *ibid.* **10A** (1979) 1808.
8. K. S. RAVICHANDRAN, *Scrita Metall.* **24** (1990) 1275.
9. *Idem.*, *Acta Metall. Mater.* **39** (1991) 401.
10. J. S. KIM, Y. W. CHANG and C. S. LEE, *Met. Mater.* **4** (1998) 771.
11. J. OH, N. J. KIM, S. LEE and E. W. LEE, *J. Mater. Sci. Lett.* **20** (2001) 2183.
12. *Idem.*, *Mater. Sci. Eng.* A **A340** (2003) 232.
13. S. SURESH, in "Fatigue of Materials," edited by S. SURESH (Cambridge Univ. Press, Cambridge, 1991) p. 226.
14. D. EYLON, S. FUJISHIRO, P. J. POSTANS and F. H. FROES, *Titanium Tech.* (1985) 87.
15. D. EYLON and J. A. HALL, *Metall. Trans.* A **8A** (1997) 981.
16. C. A. STUBBINGTON and A. W. BOWEN, *J. Mater. Sci.* **9** (1974) 941.
17. D. K. BENSON, J. C. GROSSKREUTZ and G. G. SHAW, *Metall. Trans.* A **3A** (1972) 1239.
18. D. EYLON and P. J. BANIA, *ibid.* **9A** (1978) 1273.
19. D. EYLON, *J. Mater. Sci.* **14** (1979) 1914.
20. R. C. MCCLUNG, *Fatigue Fract. Eng. Mater. Struct.* **14** (1991) 455.

Received 20 September 2002
and accepted 4 September 2003